

Short communication

Electrochemical performances of lithium-ion polymer battery using $\text{LiNi}_{1/3}\text{Co}_{1/3}\text{Mn}_{1/3}\text{O}_2$ as cathode materials

Hyun-Soo Kim^{*}, Chang-Woo Lee, Seong-In Moon

Battery Research Group, Korea Electrotechnology Research Institute, 28-1 Seongju-dong, Changwon 641-120, Korea

Available online 14 June 2006

Abstract

In this work, a gel polymer electrolyte (GPE) was prepared using polyoxyalkylene glycol acrylate (POAGA) as a macromonomer. $\text{LiNi}_{1/3}\text{Mn}_{1/3}\text{Co}_{1/3}\text{O}_2$ /GPE/graphite cells were prepared and their electrochemical properties were evaluated at various current densities and temperatures. The ionic conductivity of the GPE was more than $6.2 \times 10^{-3} \text{ S cm}^{-1}$ at room temperature. The GPE had good electrochemical stability up to 5.0 V versus Li/Li^+ . POAGA-based cells showed good electrochemical performances such as rate capability, low-temperature performance, and cycleability. No leakage of the electrolyte or an explosion was observed at the overcharge test.

© 2006 Elsevier B.V. All rights reserved.

Keywords: Macromonomer; Polyoxyalkylene glycol acrylate; Lithium ion polymer battery; Gel polymer electrolyte; Curable mixture; Ionic conductivity

1. Introduction

Lithium-ion secondary battery has been used widely as an energy source in a portable IT device since it has been commercialized in Japan in the early of 1990's. A fluid electrolyte composed of an organic solvent and lithium salt has been served a lithium conductive media in the lithium-ion battery. It may give rise to hazard when there is a leakage of the electrolyte in the battery; an organic solvent such as a dimethyl carbonate (DMC) and dimethoxy ethane (DME) is very highly inflammable. There is still a potential risk, although several safety devices have been installed in order to avoid such a danger in the commercialized lithium secondary battery. In the last few years, a considerable number of studies have been made on a lithium-ion polymer battery with a gel polymer electrolyte to lessen a possibility of the leakage and then improve the safety. There are two kinds of host polymer, a thermoplastic material and a cross-link-type monomer/oligomer, to immobilize the liquid electrolyte in the gel polymer electrolyte.

In the thermoplastic polymer system, it has been focused on poly (ethylene oxide) (PEO) [1,2], polyacrylonitrile (PAN) [3], poly (vinylidene fluoride) (PVdF) [4], poly (methylmethacrylate) (PMMA) [5], polyvinylidene fluoride - hexafluoro

propylene (PVdF-HFP) copolymer [6], and so on. A mixed solution of the electrolyte and polymer is hardly impregnated into the electrodes because its viscosity is very high in the thermoplastic polymer system. The electrolyte may also flow at the elevated temperature since the polymer does not cross-link in this system; when the electrolyte has fluidity due to the abnormal reaction in the cell, the fresh electrolyte is supplied continuously to the place where the abnormal reaction takes place.

On the other hand, a cross-linkable polymer such as tri (ethylene glycol) dimethacrylate (TEGDMA) [7], tetra (ethylene glycol) diacrylate (TEGDA) [8], polyurethane acrylate (PUA) [9,10], and so forth has been reported for the host polymer matrix; acrylate- or methacrylate-base monomer is cross-linked and used as the matrix polymer. The ionic conductivity, ca. $10^{-3} \text{ S cm}^{-1}$ at room temperature, of the gel polymer electrolyte is sufficient in the commercialized lithium battery but cycle performance is not enough yet.

It is easy to design and control the performance of the gel electrolyte with polyoxyalkylene glycol acrylate (POAGA) macromonomer, because an ethylene oxide and propylene oxide is contained; the ethylene oxide has good compatibility with the liquid electrolyte and a propylene oxide has rigidity. It is also expected that high cross-linking density can be obtained, since there are three vinyl bonds at the end. Kono et al. [11] have reported that the gel polymer electrolyte was synthesized from LiClO_4 salt and propylene carbonate (PC) and its ionic conductivity was ca. $2.5 \times 10^{-3} \text{ S cm}^{-1}$.

^{*} Corresponding author. Tel.: +82 55 280 1663; fax: +82 55 280 1590.
E-mail address: hskim@keri.re.kr (H.-S. Kim).

In this study, the gel polymer electrolyte with POAGA was synthesized and its gellation and electrochemical property were measured. And $\text{LiNi}_{1/3}\text{Mn}_{1/3}\text{Co}_{1/3}\text{O}_2$ /POAGA-base GPE/graphite cells were prepared and their electrochemical performances were also evaluated.

2. Experimental

The gel polymer electrolyte was prepared by a thermal curing for a precursor consisted of a liquid electrolyte, a monomer, and an initiator. A battery grade solution of 1.0M LiPF_6 /ethylene carbonate (EC)+propylene carbonate (PC)+ethyl methyl carbonate (EMC)+diethyl carbonate (DEC) (30:20:20:30 wt%) was obtained from Cheil Industries and used as a liquid electrolyte. Polyoxyalkylene glycol acrylate ($M_w = 11,000$) and bis (4-tert-butylcyclohexyl) peroxydicarbonate (BBP, Aldrich Chemical Co.) was used as a macromonomer and initiator, respectively. 3.0 vol% of POAGA and 2.0 wt% of BBP was mixed in the liquid electrolyte. The mixed solution was polymerized at a temperature range of 50–80 °C for 60 min. All procedures for preparing the precursor were carried out in an argon filled dry-box to avoid an effect of humidity.

The ionic conductivity of the gel polymer electrolyte was measured using an AC impedance analyzer (IM6, Zahner Elektrik) with a stainless steel blocking electrode cell. Electrode area and thickness of the electrolyte was 3.14 mm² and 0.1 mm, respectively. Ionic conductivity was measured for temperatures ranging from –20 to 60 °C. A potential difference of 5 mV was applied to the sample for frequencies ranging from 100 to 2 mHz. The electrochemical window of the GPE was studied using the technique of cyclic voltammetry (CV). CV was carried out using a potentiostat (model 273, EG&G Co.). A three-electrode system was used for all measurement. A stainless steel was used the working electrode and a lithium electrode was used as the counter and the reference electrode, respectively. A stainless steel electrode with an area of 3 cm × 5 cm was swept in the potential range of –0.5 to 5.0 V versus Li/Li⁺ at a sweep rate of 5 mV s^{–1}.

Cathodic electrode was prepared by mixing 93 wt% $\text{LiNi}_{1/3}\text{Mn}_{1/3}\text{Co}_{1/3}\text{O}_2$ with 4 wt% super P black and 3 wt% PVdF and coated on an aluminum foil. Graphite electrode was prepared using 95 wt% mesophase carbon beads (MCMB) and 5 wt% PVdF and coated on a copper foil. Celgard 2500 was used as a separator. The electrodes were stacked and inserted into an aluminum laminated film. The precursor was filled into the assembled cell in a dry-box filled with argon gas and then the cell was vacuum-sealed. The assembled cells were polymerized at 60 °C for 60 min in an oven. The fabrication procedure of the cell has been described in our previous papers [5,12].

Battery performances of the prepared lithium-ion polymer battery were examined using a battery cycler system (Maccor 3000 series) and AC impedance analyzer. Rate capability of the cells was measured at 0.2C, 0.5C, 1.0C and 2.0C rate using Maccor 3000 series. Here, symbol “C” stands for the current rate provided to cycle the cell system. 0.2C means

that the charging and discharging process takes 5 h, respectively. That is, 0.2C can be expressed as a C/5 current rate alternatively. Low-temperature performance was examined at a 0.5C rate at a temperature of –20, –10, 0 and 20 °C. The charge and discharge cycling tests of the cells were conducted galvanostatically at a 0.5C rate in a voltage range of 4.4–2.8 V. An electrochemical impedance spectroscopy of the obtained cell was evaluated using an AC impedance analyzer after charge and discharge cycling. AC impedance measurements were performed by using Zahner Elektrik IM6 impedance analyzer over a frequency range of 700 mHz to 2 MHz for interface investigation of the cells. Overcharge test was performed in a constant current regime at a 1C rate for 250 min. The test was come to an end, when the cell voltage reached to 12 V.

3. Results and discussion

Polymerization condition of POAGA-based GPE was examined using a test tube to obtain optimum polymerization temperature and time. Fig. 1 showed gellation time with a curing temperature for the GPE. As shown in the Fig. 1, gellation time decreased exponentially with increasing the curing temperature. It meant that gellation of the GPE was primary dominated by the temperature. When the content of the POAGA increased, the curing time decreased and gel was harder. Those behaviors might arise from that a cross-linking density increased with increasing the content of macromonomer.

The ionic conductivity of the GPE was measured using an AC impedance analyzer with a stainless steel blocking electrode. Fig. 2 showed the AC impedance spectra of the GPEs polymerized at temperature of 60 °C for 60 min. There was only a spike, which represents a resistor in series with a capacitor, at the plot. The intercept on the real axis gives the resistance of the GPE. The ionic conductivity at 23 °C was calculated to be $6.2 \times 10^{-3} \text{ S cm}^{-1}$ from the electrolyte resistance with thickness and surface area of the GPE. Fig. 3 showed the ionic conductivity of the GPE at various temperatures. As shown in the Fig. 3, its ionic conductivity at a temperature of –20 °C

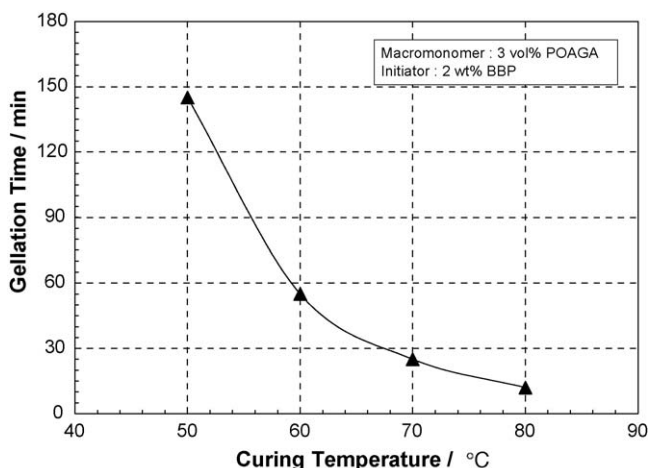


Fig. 1. Variation of gellation time of GPE with polymerization temperature.

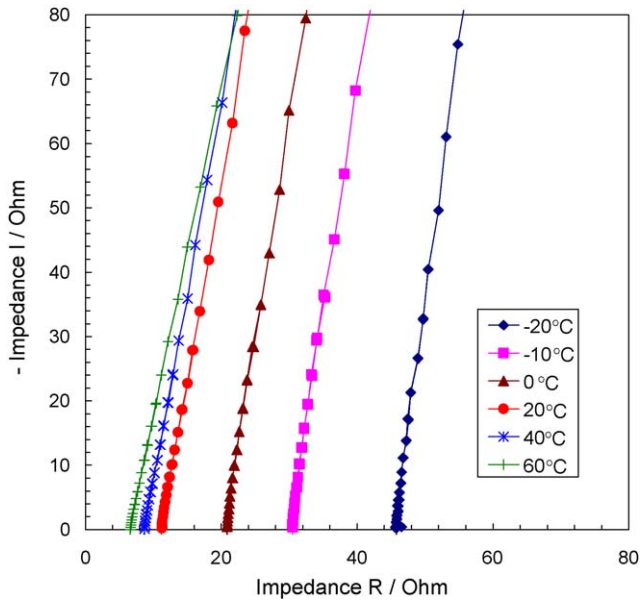


Fig. 2. AC impedance spectra of SS/GPE/SS cells with gel polymer electrolyte.

was $1.52 \times 10^{-3} \text{ S cm}^{-1}$ and increased with increasing temperature. It is thought that one of the reasons for high-conductivity is mainly due to the liquid electrolyte in the GPE; the GPE was composed of 97 vol% liquid electrolyte and 3 vol% reactive macromonomer.

The electrochemical stability window of the GPE was examined using a cyclic voltammetry and shown in Fig. 4. The cyclic voltammogram of the GPE was measured using stainless steel electrodes between -0.5 and 5.0 V versus Li/Li^+ . No peak was observed up to 5.0 V except at potential range of -0.5 – 0.5 V . Therefore, there is no problem in the electrochemical stability, because charging voltage for lithium ion battery using $\text{LiNi}_{1/3}\text{Mn}_{1/3}\text{Co}_{1/3}\text{O}_2$ material is about 4.3 – 4.6 V [13]. On scanning the electrode in a negative direction, a cathodic peak is observed at about -0.45 V , which corresponds to the plating of lithium on to the Ni electrode. On the reverse scan, stripping of lithium is observed at about 0.37 V . The voltammogram

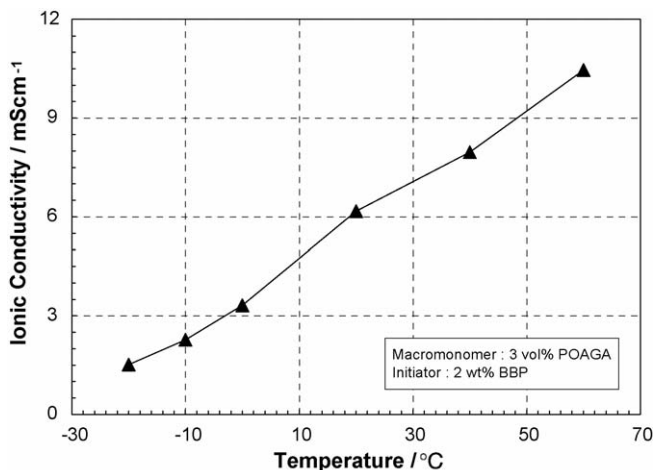


Fig. 3. Ionic conductivity of the gel polymer electrolyte at various temperatures.

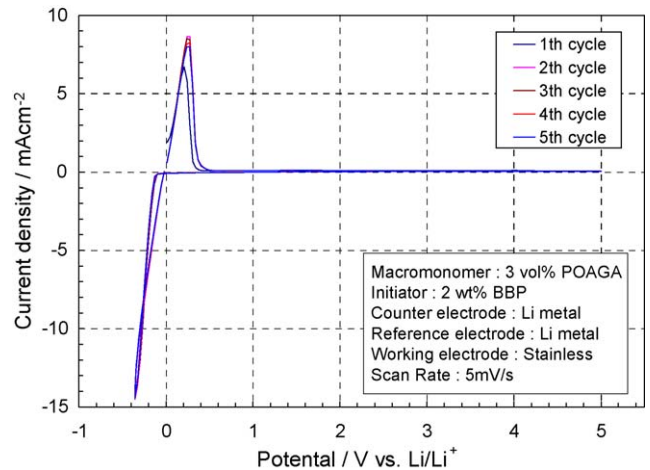


Fig. 4. Cyclic voltammograms of the gel polymer electrolyte on SS working electrode.

ascribed to lithium deposition/dissolution is highly reversible, because the peak currents remain fairly constant with repeated cycling.

In order to evaluate the electrochemical performance of a lithium-ion polymer cell using the gel polymer electrolyte, a $\text{LiNi}_{1/3}\text{Mn}_{1/3}\text{Co}_{1/3}\text{O}_2/\text{GPE}/\text{graphite}$ cell was fabricated. Open circuit potential (OCP) and impedance of the cell was measured with the manufacturing process. The value of OCP was 100 – 150 mV after aging followed by electrolyte filling and increased to 120 – 180 mV after thermal curing. Impedance of the lithium-ion polymer battery increased during a thermal curing and decreased after a pre-conditioning process. The impedance of the manufactured cell was about 30 – $35 \text{ m}\Omega$, which was similar value in the lithium secondary battery with the liquid electrolyte. However, OCP and impedance of the cells kept stable with the content of the macromonomer and initiator.

The assembled cell was preconditioned with a cut-off voltage of 4.4 V for the upper limit and 2.8 V for the lower limit at the 0.1C rate. An irreversible capacity was observed in the 1st cycle and this is caused by the formation of passivation film on the surface of the carbon electrode due to the decomposition of electrolyte, as reported previously by other authors [14,15]. The process of passivation film on the surface during the initial cycling is referred to as the formation period. The film can prevent the electrolyte from further reduction by the active lithium and thus limits the degradation of electrolytes. After the preconditioning cycle, the rate capability of the cell was evaluated. The discharge curves obtained at different current rates were given in Fig. 5. The cell delivered a discharge capacity of 164.8 mAh g^{-1} at 0.2C rate. The discharge capacity slowly decreased with current rate, which was due to polarization. A useful capacity of 159.6 mAh g^{-1} was obtained at 0.5C rate, which was 96.8% of the discharge capacity at 0.2C rate. The capacity of 146.3 mAh g^{-1} was available even at 2C rate, which was 88.8% of the discharge capacity at 0.2C rate. The reduced capacity in the $\text{LiNi}_{1/3}\text{Mn}_{1/3}\text{Co}_{1/3}\text{O}_2/\text{GPE}/\text{graphite}$ cell at high rate may be primarily related to the lower impregnation and to the lower diffusion rate of lithium ions in the gel

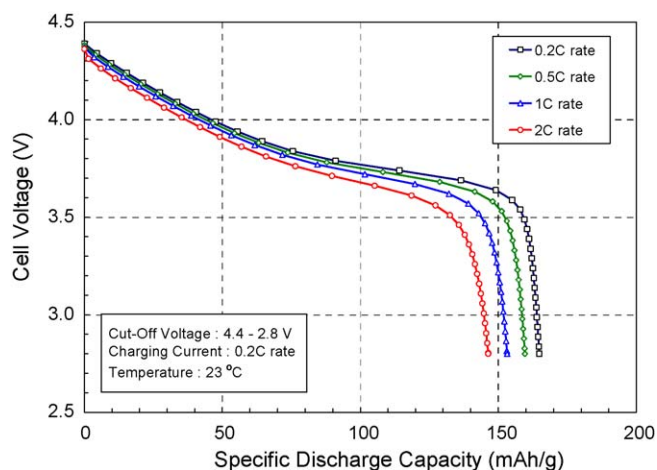


Fig. 5. Typical discharge curves obtained at various current rates for $\text{LiNi}_{1/3}\text{Mn}_{1/3}\text{Co}_{1/3}\text{O}_2/\text{GPE}/\text{graphite}$ cells at 23°C .

polymer electrolyte [16]. Further research is being conducted to improve the high-rate performance of the lithium-ion polymer batteries.

The performances of the $\text{LiNi}_{1/3}\text{Mn}_{1/3}\text{Co}_{1/3}\text{O}_2/\text{GPE}/\text{graphite}$ cell at various temperatures were also evaluated. The discharge curves obtained at 0.2C rate at various temperatures were given in Fig. 6. The discharge capacity of the cell was ca. 159.6mAh g^{-1} at 20°C . The discharge capacity slowly decreased with decreasing the temperature. A useful capacity of ca. 130.8mAh g^{-1} was obtained at -10°C , which was 82.0% of the discharge capacity at 20°C . The capacity of ca. 109.7mAh g^{-1} was available even at temperature of -20°C , which was 68.7% of the discharge capacity at 20°C . Recently, ethyl methyl carbonate (EMC) was found to be a useful co-solvent in binary solutions with propylene carbonate and ethylene carbonate because of its low freezing point (-55°C). Performances of the lithium-ion cells at low temperature can be improved using such solvents having low freezing point.

Fig. 7 showed the discharge capacity and capacity retention with cycling for $\text{LiNi}_{1/3}\text{Mn}_{1/3}\text{Co}_{1/3}\text{O}_2/\text{GPE}/\text{graphite}$ cell

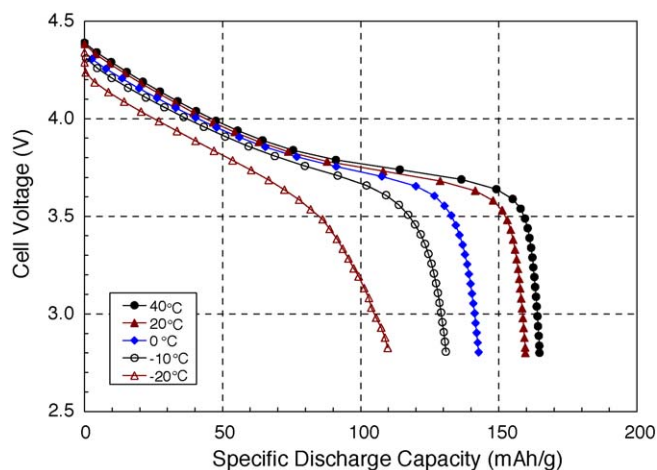


Fig. 6. Typical discharge curves obtained at 0.5C rate for $\text{LiNi}_{1/3}\text{Mn}_{1/3}\text{Co}_{1/3}\text{O}_2/\text{GPE}/\text{graphite}$ cell at various temperatures.

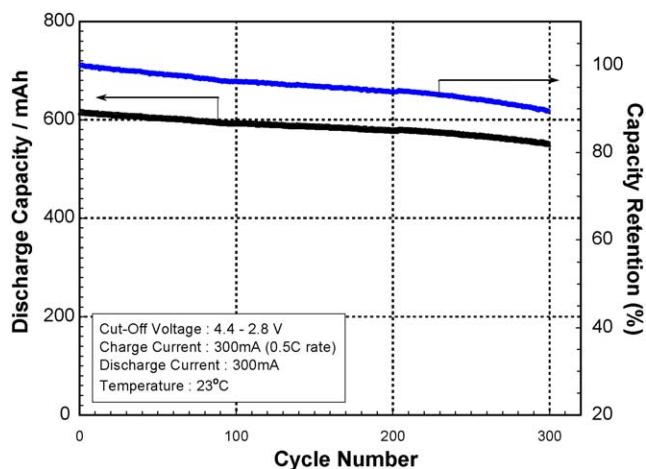


Fig. 7. Capacity change upon cycling at 1C rate for $\text{LiNi}_{1/3}\text{Mn}_{1/3}\text{Co}_{1/3}\text{O}_2/\text{GPE}/\text{graphite}$ cell at 23°C .

at 0.5C rate. Discharge capacity of the cell was stable with charge–discharge cycling; the discharge capacity was 551.4mAh after the 300th cycling, which was 89.7% of the initial capacity. It is expected that cross-linked polymer after curing decreases the interface resistance between the electrode and the GPE. After cycling test, as surface of the electrodes was observed with the naked eye, cathode was adhered closely to the separator but anode was come apart from the separator. A lithium compound was covered on the surface of the anode electrode; it seemed to deteriorate the cycleability for the cell. The $\text{LiNi}_{1/3}\text{Mn}_{1/3}\text{Co}_{1/3}\text{O}_2/\text{GPE}/\text{graphite}$ cell exhibited better cycle performance, when content of the macromonomer was high or content of the initiator is low; it was thought that high cross-linking density caused a interfacial resistance between the electrodes and GPE; an excess amount of macromonomer led to deterioration of the cycleability.

Electrochemical impedance spectra (EIS) of the $\text{LiNi}_{1/3}\text{Mn}_{1/3}\text{Co}_{1/3}\text{O}_2/\text{GPE}/\text{graphite}$ cell were depicted in Fig. 8. The impedance spectrum of the cell was obtained after filling of the precursor, 1st and 100th cycling. After 1st cycling, the impedance spectroscopy of the cell exhibited two depressed semicircles. The Z' intercept of the semicircle on the real axis at higher frequency is related to the bulk resistance (R_b) of the gel polymer electrolyte. The semicircle was assumed to be associated with a parallel combination of interfacial resistance (R_{int} electrode/electrolyte interface) and the constant-phase element of the multi-passivation films on both electrode surfaces [17]. The diameter of the semicircle is related to the interfacial resistance (R_{int}) between the electrode and the gel polymer electrolyte [18]. The semicircle at medium frequency is assigned to the parallel combination of the charge transfer resistance (R_{ct}) (as indicated by the diameter of the medium-frequency semicircle) in the electrodes and the double-layer capacitance (C_{dl}) contributed by both the cathode and the anode. At a lower frequency there is a slanted line due to solid-state diffusion of Li ions within the bulk cathode/anode materials. The electrolyte resistance (intersection of EIS curve with x -axis) and two semicircles

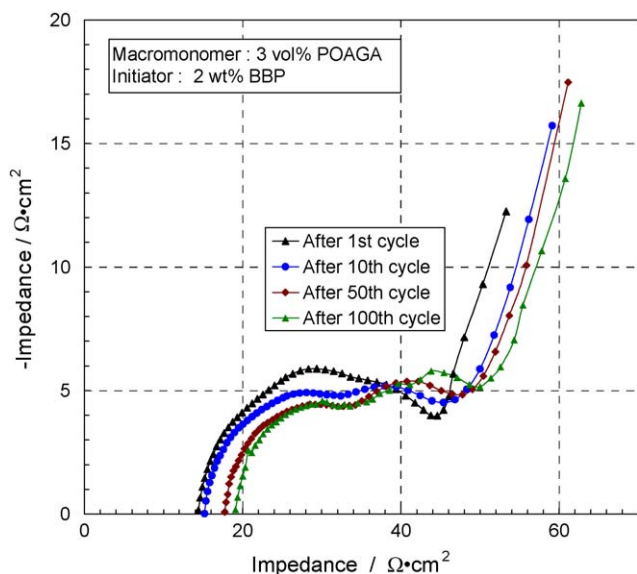


Fig. 8. AC impedance spectra of $\text{LiNi}_{1/3}\text{Mn}_{1/3}\text{Co}_{1/3}\text{O}_2/\text{GPE}/\text{graphite}$ cell at 23°C .

(which might be attributed to contact resistance and double layer capacitance due to surface film formation on active material) increased just a little during cycling for the cell. These EIS phenomena might be able to explain part of the rate capability and the cycle life characteristics of each material. The electrochemical impedance is a major part of internal resistance of a battery and the cycle life of a battery decreases as its internal resistance increases after repeated charge and discharge. Hence, the electrochemical impedance characteristics of the $\text{LiNi}_{1/3}\text{Mn}_{1/3}\text{Co}_{1/3}\text{O}_2/\text{GPE}/\text{graphite}$ cell explain the enhanced cycle life of the cell.

Safety of the lithium secondary cell is one of the important factors; especially overcharge test is indispensable to a lithium ion battery. The cell was charged with 1.0C rate for 250 min in fully discharged state. The temperature profiles related to the variation of the cell voltage were shown in Fig. 9. Typi-

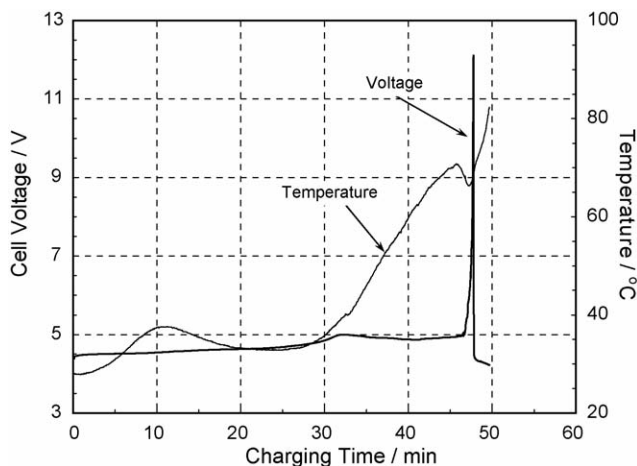


Fig. 9. Voltage and temperature profiles of lithium-ion polymer battery with overcharge test.

cally, the lithium metal is started to deposit on the surface of the anode electrode at about 4.5 V, while the electrolyte is decomposed at about 5.0 V. Here, the deposited lithium metal on the surface of the anode electrode is well known to cause a micro-short or soft-short. As shown in the Fig. 9, the cell voltage is gradually increased up to 5.0 V with charging. The surface temperature of the cell was started to increase with overcharging and then followed by decreasing the temperature at about 70°C . The temperature, at this very moment, was about 80°C and no leakage of electrolyte or an explosion was observed in the cell.

4. Conclusions

In this work, the GPE was prepared using the POAGA as a macromonomer. $\text{LiNi}_{1/3}\text{Mn}_{1/3}\text{Co}_{1/3}\text{O}_2/\text{POAGA}$ -based GPE/graphite cells were prepared and their electrochemical properties were evaluated at various current densities and temperatures. The ionic conductivity of the GPE was $6.2 \times 10^{-3} \text{ S cm}^{-1}$ at room temperature. The GPE was stable electrochemically up to 5.0 V versus Li/Li^+ . $\text{LiNi}_{1/3}\text{Mn}_{1/3}\text{Co}_{1/3}\text{O}_2/\text{POAGA}$ -based GPE/graphite cells were showed good electrochemical performances such as rate capability, low-temperature performance, and cycleability. The capacity of 146.3 mAh g^{-1} was available at 2C rate, which was 88.8% of the discharge capacity at 0.2C rate. Discharge capacity of the cell was stable with charge-discharge cycling; the discharge capacity was 551.4 mAh after the 300th cycling, which was 89.7% of the initial capacity. And no leakage of the electrolyte or an explosion was observed at the overcharge test.

Acknowledgements

This research was supported by a grant (code #: 05K1501-01910) from ‘Center for Nanostructured Materials Technology’ under ‘21st Century Frontier R&D Programs’ of the Ministry of Science and Technology, Korea

References

- [1] B. Scrosati, F. Croce, L. Persi, J. Electrochem. Soc. 147 (2000) 1718–1721.
- [2] J. Kim, S. Moon, B. Jin, H. Ku, M. Yun, J. KIEEME 8 (1995) 412–416.
- [3] K.M. Abraham, M. Alamgir, J. Electrochem. Soc. 137 (1990) L1657–L1663.
- [4] F. Boudin, X. Andrieu, C. Jehoulet, I.I. Olsen, J. Power Sources 81–82 (1999) 804–807.
- [5] H. Kim, J. Shin, S. Moon, S. Kim, Electrochim. Acta 48–11 (2003) 1573–1578.
- [6] V. Arcella, A. Sanguineti, E. Quartane, P. Mustarelli, J. Power Sources 81–82 (1999) 790–794.
- [7] H. Kim, J. Shin, C. Doh, S. Moon, S. Kim, J. Power Sources 112 (2002) 469–476.
- [8] H. Kim, J. Shin, S. Moon, M. Yun, J. Power Sources 119–121 (2003) 482–486.
- [9] H. Kim, G. Choi, S. Moon, S. Kim, J. Appl. Electrochem. 33 (2003) 491–496.
- [10] H. Kim, S. Kim, G. Choi, S. Moon, S. Kim, J. KIEEME 15 (2002) 1033–1038.

- [11] M. Kono, E. Hayashi, M. Watanabe, *J. Electrochem. Soc.* 146 (1999) 1626–1632.
- [12] H. Kim, S. Kim, G. Choi, S. Moon, S. Kim, *J. Korean Electrochem. Soc.* 5 (2002) 197–201.
- [13] H. Kim, J. Shin, S. Moon, D. Oh, *J. KIEEME* 17 (2004) 608–614.
- [14] R. Fong, U. von Sacken, J.R. Dahn, *J. Electrochem. Soc.* 137 (1990) 2009–2013.
- [15] J.M. Rarascon, D. Guyomard, *J. Electrochem. Soc.* 138 (1991) 2864–2868.
- [16] D.W. Kim, *J. Power Sources* 87 (2000) 78–83.
- [17] M.D. Levi, G. Salitra, B. Makovsky, H.D. Abache, U. Heider, L. Heider, *J. Electrochem. Soc.* 146 (1999) 1279–1289.
- [18] H. Wang, H. Huang, S.L. Wunder, *J. Electrochem. Soc.* 147 (2000) 2853–2861.